CrystEngComm

ROYAL SOCIETY OF CHEMISTRY

PAPER

View Article Online
View Journal | View Issue

Cite this: *CrystEngComm*, 2024, **26**, 6739

Intrinsically chiral paddlewheel diruthenium complexes†

Isabel Coloma,[a] Santiago Herrero [ab] and Miguel Cortijo *[a]

A family of heteroleptic paddlewheel diruthenium complexes has been designed to obtain a chiral arrangement of the donor atoms of their equatorial ligands around the metal–metal bond axis. In order to do so, the non-symmetric ligands 2-hydroxy-6-methylpyridinate (hmp) and 2-amino-6-methylpyridinate (amp) were employed to obtain the following four axially chiral compounds: *cis*-[$Ru_2Cl(\mu\text{-DPhF})_2(\mu\text{-hmp})(\mu\text{-OAc})$] (**Ruhmp**), *cis*-[$Ru_2Cl(\mu\text{-DPhF})_2(\mu\text{-amp})(\mu\text{-OAc})$] (**Ruamp**), *cis*-[$Ru_2Cl(\mu\text{-DAniF})_2(\mu\text{-hmp})(\mu\text{-OAc})$] (**Ru′hmp**) and *cis*-[$Ru_2Cl(\mu\text{-DAniF})_2(\mu\text{-amp})(\mu\text{-OAc})$] (**Ru′amp**) (DPhF = *N*,*N*′-diphenylformamidinate, DAniF = *N*,*N*′-bis(*p*-methoxyphenyl)formamidinate). All the compounds were studied by single crystal X-ray diffraction, confirming that a racemic mixture containing only one of the two possible regioisomers was obtained in all cases. A general nomenclature system for naming the full configuration of intrinsically chiral paddlewheel molecules is proposed using the *C*/*A* convention. In addition, electronic spectroscopy and cyclic voltamperometry data demonstrate the electronic tunable nature of this new platform. Overall, these results provide a novel example of robust and tunable chirality, which is of potential interest to be further exploited.

Received 11th October 2024,
Accepted 12th November 2024

DOI: 10.1039/d4ce01040j

rsc.li/crystengcomm

Introduction

The synthesis of chiral complexes is one of the most active topics in coordination chemistry, mainly driven by their potential applications as catalysts in asymmetric transformations in the search for enantiopure organic products.[1,2] Most of these catalysts are formed by carefully tailored chiral ligands, prepared from enantiopure reagents, that *impart* their chirality to the coordination sphere or, in other words, create distinguishable faces to be attacked by a chemical reagent, directing the orientation of substrates at the metal atoms. Alternatively, chiral complexes presenting stereogenic metal atoms[1,3–8] have been less studied as the isolation of enantiopure compounds of this type relies on chromatographic separations, derivatization strategies, or serendipitous spontaneous resolution upon crystallization.[9–14] While chirality arising from stereogenic carbon atoms is usually kept under ambient conditions, *i.e.*, no bond cleavage followed by bond formation is expected, more care should be taken with some chiral-at-metal complexes since bonds between metal atoms and ligand donor atoms are substantially more labile. Thus, the examples of configurationally stable scaffolds are typically limited to some octahedral compounds with at least three different monodentate ligands or with three or two *cis* chelate rings, some heteroleptic pseudo-tetrahedral complexes or polynuclear compounds in which the ligands adopt a helical disposition around the metal centers.[1,15–18]

Here, we turn our attention to the paddlewheel motif, a bi- or polynuclear unit supported by four bidentate bridging ligands at the equatorial positions and two, one, or no ligands at the axial positions. Among this class of compounds, diruthenium complexes have been particularly studied in detail in the last decades, mainly because of the wide variety of magnetic and electronic properties that they can display.[19–25] Additionally, some recent contributions have demonstrated that some of these complexes bearing chiral carboxylates or amidates can catalyze hetero-Diels–Alder, intramolecular C–H amination and olefin cyclopropanation reactions with remarkable asymmetric induction and high activity and stability, making them a promising alternative to the well-established dirhodium counterparts.[26–28]

Most diruthenium paddlewheel complexes are formed by average valence Ru_2^{5+} units bridged by four identical mononegative equatorial ligands and one halide or

[a] *MatMoPol Research Group, Inorganic Chemistry Department, Faculty of Chemical Sciences, Complutense University of Madrid, E-28040 Madrid, Spain.*
E-mail: miguelcortijomontes@ucm.es
[b] *Knowledge Technology Institute, Campus de Somosaguas, Complutense University of Madrid, E-28223 Pozuelo de Alarcón, Madrid, Spain*

† Electronic supplementary information (ESI) available: S1. Mass spectrometry. S2. Infrared spectroscopy. S3. Single crystal X-ray diffraction. S4. Magnetic measurements. S5. Procedure employed to assign polyhedral symbol, coordination index, configuration number and chirality symbol to coordination compounds with paddlewheel structure. CCDC 2384530–2384533. For ESI and crystallographic data in CIF or other electronic format see DOI: **https://doi.org/10.1039/d4ce01040j**

pseudohalide ligand at one axial position. The typical starting material to prepare this type of compounds is $[Ru_2Cl(\mu\text{-}OAc)_4]$, from which the acetate ligands can be replaced by other carboxylates but also amidate, amidinate, aminopyridinate, or hydroxypyridinate ligands.[19–22] Nevertheless, partial substitution of some of the acetate ligands can be achieved in a controlled manner by a fine control of the synthetic conditions.[29] Particularly, the substitution of two acetate ligands in $[Ru_2Cl(\mu\text{-}OAc)_4]$ by two formamidinate ligands, generally leads to $[Ru_2Cl(\mu\text{-formamidinate})_2(\mu\text{-}OAc)_2]$ compounds with *cis* configuration.[29] Nevertheless, *trans* complexes are also obtained when there is a high steric hindrance around the bimetallic unit.[30]

In the present work, we study the controlled replacement of only one acetate from an achiral *cis*-$[Ru_2Cl(\mu\text{-formamidinate})_2(\mu\text{-}OAc)_2]$ unit by a non-symmetric achiral ligand, leading to a chiral unit, in which the arrangement of the donor atoms of the ligands around the rigid diruthenium bond generates a stereogenic axis. Four different isomers (i–iv, with i–ii and iii–iv being two pairs of enantiomers) could be expected from the above-mentioned reaction (Fig. 1a). The ligands employed are shown in Fig. 1b and c. The resulting diruthenium scaffold is axially chiral even if the equatorial ligands present an eclipsed conformation. It should be noted that there are only few examples of heteroleptic diruthenium complexes bearing three different equatorial ligands reported in the literature,[31] and the compounds herein presented are the first axially chiral diruthenium complexes reported in the literature to the best of our knowledge.

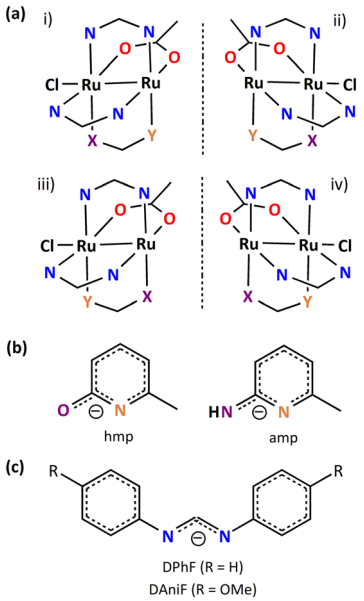

Fig. 1 (a) Simplified representation of the diruthenium core of the four possible chiral isomers (i–iv) that could be expected from the replacement of one acetate ligand in a *cis*-$[Ru_2Cl(\mu\text{-formamidinate})_2(\mu\text{-}OAc)_2]$ compound by a non-symmetric ligand. (b) Non-symmetric ligands employed: 2-hydroxy-6-methylpyridinate (hmp) and 2-amino-6-methylpyridinate (amp). (c) *N*,*N*′-diarylformamidinate ligands employed: *N*,*N*′-diphenylformamidinate (DPhF) and *N*,*N*′-bis(*p*-methoxyphenyl)formamidinate (DAniF).

Axial chirality has been thoroughly studied in organic molecules such as allenes, which present cumulated double bonds, or biphenyl, binaphthyl and related species, arising from two perpendicular non-symmetrical planes that cannot rotate freely respective to each other.[32–34] However, axial chirality has been relatively unexplored in the Inorganic Chemistry field, especially when it leads to chiral-at-metal species. Moreover, the axial chirality herein presented has a different origin since it would be retained even if a free rotation were possible.

Experimental

Materials and methods

All the chemicals were purchased from commercial sources and employed as received except for *N*,*N*′-diphenylformamidine that was recrystallized in dichloromethane/hexane. $[Ru_2Cl(\mu\text{-DAniF})_2(\mu\text{-}OAc)_2]$ was prepared modifying a published procedure to avoid the use of benzene.[30] Thin layer chromatography (TLC) analysis for the final complexes was performed using silica gel plates and a 10 : 1 chloroform/methanol mixture as eluent. FT-IR spectra were recorded using a PerkinElmer Spectrum 100 instrument with a universal ATR accessory. Mass spectra (ESI) were collected employing an ion trap-Bruker Esquire-LC Spectrometer. Fig. S1 and S2† show the mass spectra obtained for the starting materials *cis*-$[Ru_2Cl(\mu\text{-DPhF})_2(\mu\text{-}OAc)_2]$ and *cis*-$[Ru_2Cl(\mu\text{-DAniF})_2(\mu\text{-}OAc)_2]$. Elemental analyses were performed by the Microanalytical Service of Complutense University of Madrid. Electronic spectra of $\sim 10^{-4}$ M dichloromethane solutions of the complexes were recorded employing a Cary 5G spectrometer. Cyclic voltammetry measurements were carried out on a Metrohm Autolab PGSTAT204 potentiostat in a degassed tetrabutylammonium perchlorate 0.05 M dichloromethane solution. The scan rate employed was 0.1 V s^{-1} and three electrodes were used: glassy-carbon as working-electrode, Pt-wire as auxiliary electrode and Ag/AgCl as reference electrode. A ferrocene dichloromethane solution TBAP 0.05 M was used as a reference, observing the couple ferrocenium/ferrocene at 0.56 V. Single crystals of **Ruhmp**, **Ruamp**·Et_2O and **Ru′hmp** were measured employing a D8 venture diffractometer with Cu K_α radiation (λ = 1.54178 Å) in the X-ray Diffraction Service of Complutense University of Madrid. **Ru′amp**·$0.5C_6H_{12}$ crystal was measured using a Rigaku Synergy-R diffractometer with Cu K_α radiation (λ = 1.54178 Å) in the X-ray Diffraction Service the Autonomous University of Madrid. CCDC 2384530–2384533 contain the crystallographic data for this work. Structures were solved employing Olex2 software[35] with SHELXT structure solution program using intrinsic phasing[36] and refined with the SHELXL using least squares minimization.[37] Non-hydrogen atoms were refined

anisotropically, while hydrogen atoms were included with fixed isotropic contributions at their calculated positions. The methoxy group and one aromatic ring of a DAniF ligand in the structure of **Ru′amp**·$0.5C_6H_{12}$ was split into two positions with refined occupancies of 0.48 and 0.52. In addition, a disordered cyclohexane molecule, with a chemical occupancy of 0.5, was found in the asymmetric unit of **Ru′amp**·$0.5C_6H_{12}$. Consequently, three carbon atoms of this molecule were split into two positions with 0.298 and 0.202 refined occupancies. Magnetization measurements at variable temperature were carried out using a Quantum Design MPMXL SQUID magnetometer, under a 0.5 T magnetic field, employing 15.01, 7.42, 16.63, and 18.56 mg of **Ruhmp**, **Ruamp**, **Ru′hmp** or **Ru′amp**. The data were corrected for the diamagnetic contribution of the sample holder and the compounds.

Synthesis of *cis*-[$Ru_2Cl(\mu\text{-}DPhF)_2(\mu\text{-}OAc)_2$]

A mixture of [$Ru_2Cl(\mu\text{-}OAc)_4$] (0.50 g, 1.06 mmol), *N*,*N*′-diphenylformamidine (HDPhF) (0.31 g, 1.58 mmol), LiCl (0.50 g, 11.79 mmol) and Et_3N (0.35 mL, 1.88 mmol) was heated overnight in 50 mL of refluxing acetone. The mixture was filtered, the solid was dissolved in 30 mL of CH_2Cl_2 and filtered. The solution was washed with 3 × 50 mL of distilled water. The organic phase was dried over magnesium sulfate, filtered and taken to dryness, obtaining a purple solid. Yield: 54% (0.34 g). Elemental analysis for $C_{30}H_{28}ClN_4O_4Ru_2{\cdot}1.5H_2O{\cdot}0.25CH_2Cl_2$ (794.431 g mol^{-1}): % found (theoretical); C, 45.81 (45.74); H, 3.98 (4.00); N, 6.94 (7.05). IR: $\tilde{\nu}$ (cm^{-1}) = 3056 w, 3033 w, 2963 w, 1690 w, 1634 w, 1593 w, 1521 s, 1485 s, 1431 s, 1350 m, 1310 s, 1212 s, 1155 m, 1076 m, 1045 m, 1026 m, 1003 w, 941 m, 906 w, 842 w, 776 m, 757 s, 729 m, 690 s, 621 m. MS (ESI^+): *m*/*z* = 712.0, $[M–Cl]^+$ (100%).

Synthesis of *cis*-[$Ru_2Cl(\mu\text{-}DAniF)_2(\mu\text{-}OAc)_2$]

A mixture of [$Ru_2Cl(\mu\text{-}OAc)_4$] (1.00 g, 2.12 mmol), *N*,*N*′-bis(*p*-methoxyphenyl)formamidine (HDAniF) (0.81 g, 3.18 mmol), LiCl (1.00 g, 23.58 mmol) and Et_3N (0.63 mL, 3.38 mmol) was heated overnight in 120 mL of refluxing THF. The solvent was evaporated and the resulting residue redissolved in 300 mL of toluene and filtered through Celite®. The blue product was precipitated with 300 mL of hexane, filtered and dried under vacuum. Yield: 42% (0.60 g). Elemental analysis for $C_{34}H_{36}ClN_4O_8Ru_2{\cdot}2.5H_2O$ (911.319 g mol^{-1}): % found (theoretical); C, 44.69 (44.81); H, 4.41 (4.53); N, 6.24 (6.15). IR: $\tilde{\nu}$ (cm^{-1}) = 3381 w, 3083 w, 3009 w, 2929 w, 2832 w, 1636 w, 1605 m, 1579 w, 1532 m, 1498 vs, 1471 m, 1440 s, 1348 m, 1321 m, 1291 m, 1242 s, 1212 vs, 1174, 1112 m, 1022 s, 949 m, 828 s, 791 m, 786 m, 729 m, 691 s, 642 m, 617 m, 594 s. MS (ESI^+): *m*/*z* = 832.1, $[M–Cl]^+$ (100%); 909.1, $[M + CH_3CO]^+$ (6%).

Synthesis of *cis*-[$Ru_2Cl(\mu\text{-}DPhF)_2(\mu\text{-}hmp)(\mu\text{-}OAc)$] (Ruhmp)

A mixture of [$Ru_2Cl(\mu\text{-}DPhF)_2(\mu\text{-}OAc)_2$] (0.50 g, 0.67 mmol) and 2-hydroxy-6-methylaminopyridine (Hhmp) (0.15 g, 1.34 mmol) was heated in 200 mL of refluxing THF overnight. The reaction mixture was filtered, and the solvent evaporated. The solid obtained was washed with a 1 : 6 mixture of THF/water (200 mL). The solid was dissolved in CH_2Cl_2, and the solution was dried over magnesium sulfate and filtered. The solvent was evaporated under vacuum obtaining a purple-pinkish solid. TLC in silica gel; eluent (v/v): chloroform/methanol (10 : 1): 1 spot (Rf = 0.25). Yield: 71% (0.42 g). Elemental analysis for $C_{34}H_{31}ClN_5O_3Ru_2{\cdot}CH_2Cl_2$ (880.183 g mol^{-1}): % found (theoretical); C, 47.43 (47.76); H, 3.78 (3.78); N, 7.89 (7.96). IR: $\tilde{\nu}$ (cm^{-1}) = 3053 w, 2965 w, 2904 w, 1709 w, 1614 m, 1594 m, 1526 s, 1487 s, 1441 m, 1425 s, 1380 m, 1365 m, 1323 s, 1260 m, 1217s, 1174 m, 1158 m, 1080 m, 1027 s, 1015 s, 945 m, 910 w, 883 m, 797 s, 773 s, 756 s, 690 vs, 660 m, 627 m, 589 m. UV/vis-NIR (CH_2Cl_2): λ_{max} (ε/M^{-1} cm^{-1}) = ~360 sh (4300), 505 (3800), 627 (2600) nm. MS (ESI^+): *m*/*z* = 761.1, $[M–Cl]^+$ (100%). Single crystals of **Ruhmp** were obtained by vapor diffusion of Et_2O in a solution of the complex in $CHCl_3$.

Synthesis of *cis*-[$Ru_2Cl(\mu\text{-}DPhF)_2(\mu\text{-}amp)(\mu\text{-}OAc)$] (Ruamp)

[$Ru_2Cl(\mu\text{-}DPhF)_2(\mu\text{-}OAc)_2$] (0.50 g, 0.67 mmol) and 2-amino-6-methylaminopyridine (Hamp) (0.15 g, 1.34 mmol) were heated overnight in 200 mL of refluxing THF. Then, the mixture was filtered, and the solvent evaporated. The solid obtained was washed with 60 mL of a 1 : 6 mixture of THF/water. The product was dissolved in CH_2Cl_2, and the solution was dried over magnesium sulfate and filtered. The solvent was evaporated obtaining a dark blue solid. TLC in silica gel; eluent (v/v): chloroform/methanol (10 : 1): 1 spot (Rf = 0.50). Yield: 87% (0.47 g). Elemental analysis for $C_{34}H_{32}ClN_6O_2Ru_2{\cdot}0.25H_2O$ (798.769 g mol^{-1}): % found (theoretical); C, 51.16 (51.13); H, 4.03 (4.10); N, 10.48 (10.52). IR: $\tilde{\nu}$ (cm^{-1}) = 3386 w, 3271 w, 3055 w, 3033 w, 2963 w, 2908 w, 1607 m, 1594 m, 1534 s, 1486 s, 1471 s, 1431 m, 1392 m, 1348 m, 1216 s, 1165 m, 1076 m, 1026 m, 1010 m, 943 m, 915 m, 889 m, 843 m, 801 m, 783 m, 770 s, 756 s, 729 m, 690 vs, 661 s, 619 m, 598 m, 578 m. UV/vis-NIR (CH_2Cl_2): λ_{max} (ε/M^{-1} cm^{-1}) = ~347 sh (6300), 437 (2200), ~527 sh (3300), 585 (4400), ~663 sh (2600), 924 (1000) nm. MS (ESI^+): *m*/*z* = 760.2, $[M–Cl]^+$ (100%). Single crystals of **Ruamp**·Et_2O were obtained by vapor diffusion of Et_2O in a solution of the complex in $CHCl_3$.

Synthesis of *cis*-[$Ru_2Cl(\mu\text{-}DAniF)_2(\mu\text{-}hmp)(\mu\text{-}OAc)$] (Ru′hmp)

A mixture of [$Ru_2Cl(\mu\text{-}DAniF)_2(\mu\text{-}OAc)_2$] (0.50 g, 0.58 mmol), 2-hydroxy-6-methylaminopyridine (Hhmp) (0.13 g, 1.15 mmol) was heated in 200 mL of refluxing THF overnight. Then, the reaction mixture was filtered, and the solvent was evaporated under vacuum. The resulting solid was washed with 100 mL of distilled water and dissolved in CH_2Cl_2. The solution was dried over magnesium sulfate and filtered. The solvent was evaporated under vacuum obtaining a purple product. TLC in silica gel; eluent (v/v): chloroform/methanol (10 : 1): 1 spot (Rf = 0.37). Yield: 71% (0.38 g). Elemental analysis for $C_{38}H_{39}ClN_5O_7Ru_2$ (915.356 g mol^{-1}): % found

(theoretical); C, 50.16 (49.86); H, 4.27 (4.29); N, 7.56 (7.65). IR: $\tilde{\nu}$ (cm^{-1}) = 3038 w, 2995 w, 2949 w, 2932 w, 2908 w, 2835 w, 1638 w, 1606 m, 1580 w, 1546 w, 1531 m, 1498 vs, 1439 s, 1381 m, 1365 m, 1315 m, 1292 m, 1242 s, 1211 vs, 1168 s, 1106 m, 1026 s, 947 m, 828 s, 790 m, 767 m, 727 m, 690 s, 643 m, 621 m, 593 m. UV/vis-NIR (CH_2Cl_2): λ_{max} (ε/M^{-1} cm^{-1}) = ~379 sh (5700), 509 (4400), 668 (3300) nm. MS (ESI^+): m/z = 881.1, $[M–Cl]^+$ (100%). Single crystals of **Ru′hmp** were obtained by slow diffusion of cyclohexane in a THF solution of the complex.

Synthesis of *cis*-[$Ru_2Cl(\mu$-DAniF$)_2(\mu$-amp$)(\mu$-OAc$)$] (**Ru′amp**)

[$Ru_2Cl(\mu$-DAniF$)_2(\mu$-OAc$)_2$] (0.50 g, 0.58 mmol), 2-amino-6-methylaminopyridine (Hamp) (0.13 g, 1.15 mmol) and 200 mL of THF were added to a Schlenk flask. The mixture was heated under reflux overnight and filtered. The solution was taken to dryness and the blue solid obtained was washed with abundant distilled water. Then, the solid was dissolved in CH_2Cl_2, and the solution was washed with more water. The organic phase was dried over magnesium sulfate, filtered and evaporated. TLC in silica gel; eluent (v/v): chloroform/methanol (10 : 1): 1 spot (Rf = 0.38). Yield: 88% (0.51 g). Elemental analysis for $C_{38}H_{40}ClN_6O_6Ru_2{\cdot}CH_2Cl_2$ (999.305 g mol^{-1}): % found (theoretical); C, 46.84 (46.88); H, 4.33 (4.24); N, 8.12 (8.41). IR: $\tilde{\nu}$ (cm^{-1}) = 3265 w, 3036 w, 2997 w, 2951 w, 2908 w, 2835 w, 1607 m, 1539 m, 1499 vs, 1476 s, 1439 m, 1392 m, 1349 w, 1317 m, 1292 m, 1242 s, 1213 s, 1168 s, 1105 w, 1028 s, 945 m, 828 s, 804 m, 790 m, 768 m, 727 m, 689 m, 643 m, 620 m, 593 m. UV/vis-NIR (CH_2Cl_2): λ_{max} (ε/M^{-1} cm^{-1}) = ~352 sh (6700), ~377 sh (4600), 448 (2700), ~538 sh (3200), 610 (4700), ~675 sh (3100), 912 (1000) nm. MS (ESI^+): m/z = 880.2, $[M–Cl]^+$ (100%). Single crystals of **Ru′amp**·$0.5C_6H_{12}$ were obtained by slow diffusion of cyclohexane in a THF solution of the complex.

Results and discussion

The reaction of *cis*-[$Ru_2Cl(\mu$-DPhF$)_2(\mu$-OAc$)_2$] or *cis*-[$Ru_2Cl(\mu$-DAniF$)_2(\mu$-OAc$)_2$] with 2-hydroxy-6-methylpyridine (Hhmp) in refluxing THF led to the formation of **Ruhmp** or **Ru′hmp** with a 71% yield in both cases. The reaction of the same starting materials with 2-amino-6-methylpyridinate (Hamp) in the same conditions led to obtaining **Ruamp** and **Ru′amp** with yields of 87% and 88%, respectively. This fact has been confirmed by elemental analyses and the presence of the $[M–Cl]^+$ fragment in their ESI^+ spectra (see Fig. S3–S6†).

The infrared spectra of the four final compounds are shown in the ESI† (Fig. S7). Fig. S8† shows the spectra of *cis*-[$Ru_2Cl(\mu$-DAniF$)_2(\mu$-OAc$)_2$], **Ru′hmp** and **Ru′amp** in the 1800–800 cm^{-1} region, which were employed to check if the progress of these reactions can be monitored by IR spectroscopy. The O–C–O stretching bands of the acetate ligands of *cis*-[$Ru_2Cl(\mu$-DAniF$)_2(\mu$-OAc$)_2$] were found at 1440 and 1321 cm^{-1}. The intensity of these bands is smaller in the spectra of **Ru′hmp** and **Ru′amp**, which indicates the replacement of a single acetate ligand from the starting material. The same effect is observed in the IR spectra of the complexes that contain the DPhF ligand.

The IR spectra of the complexes that contain the same formamidinate ligand, but different non-symmetric bridging ligand, is almost identical. Nevertheless, the presence of amp can be identified by the N–H stretching band at ~3270 cm^{-1}. Fig. S9† show the comparison between the spectra of **Ruhmp** and **Ruamp**. More differences are found when comparing the spectra of compounds with the same non-symmetric equatorial ligand but different formamidinates. A comparison between the spectra of **Ruhmp** and **Ru′hmp**, where these differences can be observed, is shown in Fig. S10.† The first main difference is observed in the region of the aliphatic C–H stretches, due to the presence of the methoxy groups of DAniF ligands. Moreover the C–O stretching vibration bands can be observed around 1240 and 1169 cm^{-1}.[38]

The non-symmetric ligands employed were chosen because they are formed by a rigid pyridine ring and contain a methyl group at their 6th position. The presence of an axial chloride ligand in the starting material together with the presence of this methyl group in one of the sides on the non-symmetric ligands hinders the replacement of the two acetates of the *cis*-[$Ru_2Cl(\mu$-formamidinate$)_2(\mu$-OAc$)_2$] complexes employed. In fact, although a twofold excess of the ligands was employed in the syntheses, the mass spectra of the untreated reaction mixtures did not contain any trace of fragments ascribed to potential disubstituted products. In addition, and most likely ascribed to the same reason, only one of the two possible regioisomers was obtained (the mixture of enantiomers i and ii in Fig. 1a), as confirmed by thin-layer chromatography and single crystal X-ray diffraction. The reactions were also carried out under stoichiometric conditions leading to the same products but in lower yields.

Single crystals of **Ruhmp** and **Ruamp**·Et_2O were obtained by vapor diffusion of diethyl ether in a solution of the corresponding compound in chloroform while crystals of **Ru′hmp** and **Ru′amp**·$0.5C_6H_{12}$ were obtained by slow diffusion of cyclohexane in a solution of the compounds in tetrahydrofuran. They crystallize in the $P2_1/n$ space group except **Ru′amp**·$0.5C_6H_{12}$, which crystallizes in the $P\bar{1}$ space group (see Tables S1–S4† for more detailed information). The crystal structure determinations confirmed that all the compounds obtained exhibit a paddlewheel structure in which the spatial arrangement of the donor atoms of the ligands about the metal–metal axis is not superimposable on its mirror image (see Fig. 2). In all cases, the Ru1 atom exhibits octahedral geometry with the chloride axial ligand and the Ru2 atom in the axial positions. The equatorial positions are occupied by two N atoms from two different formamidinate ligands in *cis* configuration, one O from the acetate ligand and either one N (amp) or one O atom (hmp) from the non-symmetric ligand. Regarding the Ru2 atom, it presents a square pyramidal geometry, with the Ru1 atom at the apical position. The rest of the coordination sphere is

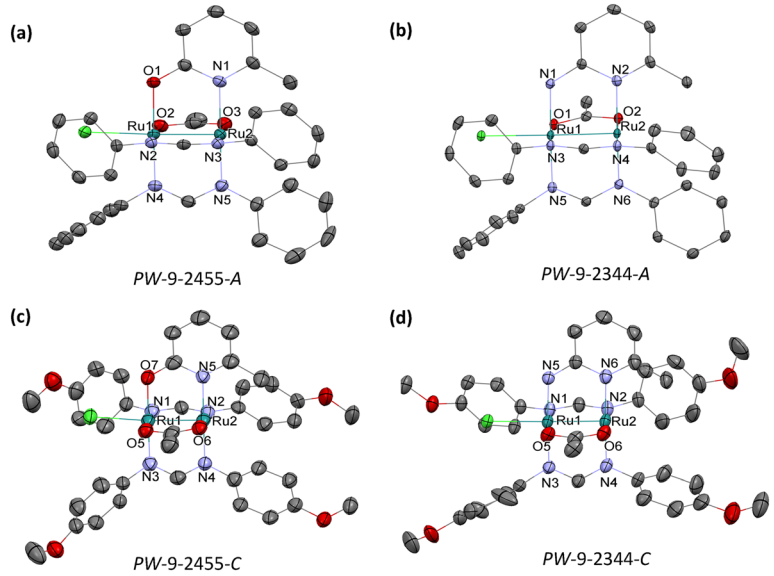

Fig. 2 Thermal ellipsoid plot of the asymmetric unit of (a) **Ruhmp**, (b) **Ruamp**, (c) **Ru′hmp**, and (d) **Ru′amp**. C atoms are depicted in grey, Cl in green, Ru in turquoise, N in purple and O in red. Ellipsoids are shown at the 50% probability level. H atoms and solvent crystallization molecules have been omitted for clarity. Fig. 2a and b show the *A* enantiomer of **Ruhmp** and **Ruamp**, Fig. 2c and d show the *C* enantiomer of **Ru′hmp** and **Ru′amp**.

formed by one O atom from the acetate and three N atoms, two from the formamidinate ligands and the other one from the non-symmetric ligand (hmp or amp). The Ru–Ru distances are 2.3098(4) Å for **Ruhmp**, 2.3076(2) Å for **Ru′amp**, 2.3093(3) Å for **Ru′hmp** and 2.3024(3) Å for **Ru′amp**, all of them typical of a metal–metal bond order of 2.5.[21] All the diruthenium units present a nearly eclipsed conformation with very small O–Ru–Ru–O, N–Ru–Ru–N and N–Ru–Ru–O torsion angles, in the 0.34–4.91° range. Fig. 2 shows a representation of the asymmetric unit of the four crystal structures. In order to

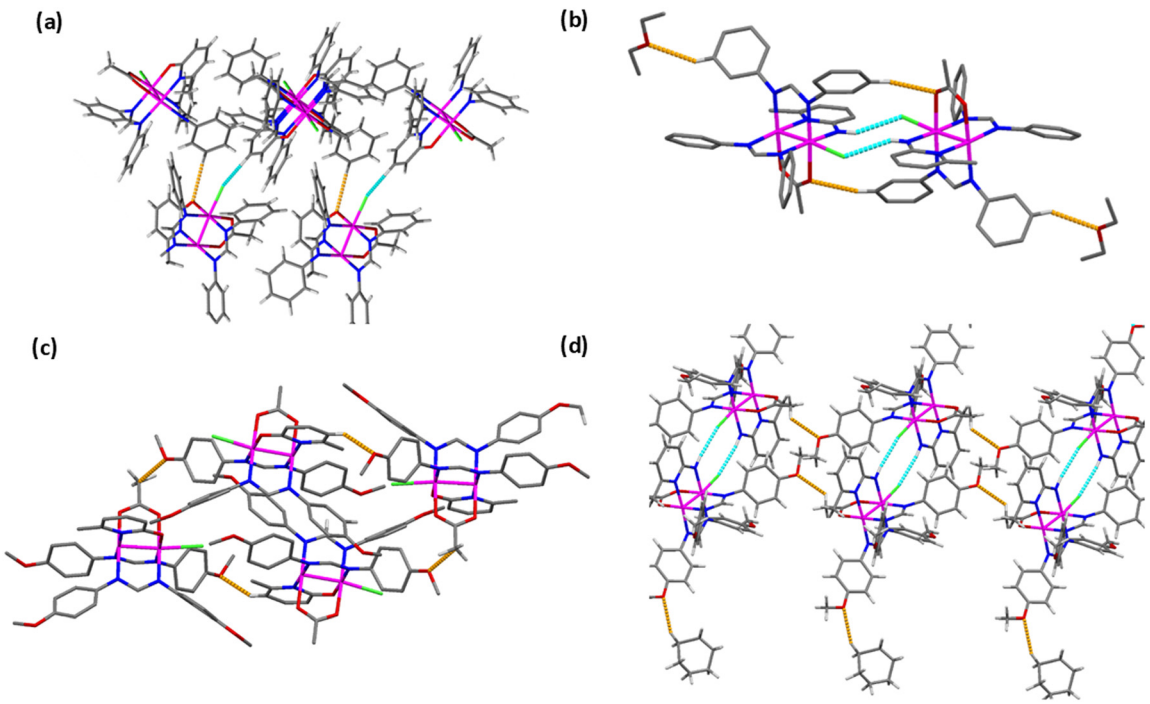

Fig. 3 (a) C–H···Cl (light blue) and C–H···O interactions (orange) between diruthenium molecules found in the crystal structure of (a) **Ruhmp**, (b) **Ruamp**·Et_2O (c) **Ru′hmp**, and (d) **Ru′amp**·0.5C_6H_{12}. H atoms not involved in the interactions are omitted for the sake of clarity. C atoms are depicted in grey, Cl in green, Ru in pink, N in blue and O in red.

name the enantiomers of these binuclear complexes, the *C*/*A* convention has been employed. A detailed description of the procedure to assign the polyhedral symbol, coordination index, configuration number and chirality symbol for binuclear paddlewheel complexes is proposed in the Supplementary Material. Accordingly, the whole configuration of the molecules shown in Fig. 2 is described as *PW*-9-2455-*A* for **Ruhmp**, *PW*-9-2344-*A* for **Ruamp**, *PW*-9-2455-*C* for **Ru′hmp**, and *PW*-9-2344-*C* for **Ru′amp**.

Fig. 3 shows the most relevant supramolecular interactions found in the four crystal structures. Each diruthenium unit interacts with two neighboring molecules through C–H···Cl and C–H···O interactions in the structure of **Ruhmp** (Fig. 3a). The C–H···Cl interactions are established between the chloride ligand of a diruthenium unit and a formamidinate ligand of the neighboring unit (2.913 Å), and the C–H···O interactions are established between the O atom of the hmp ligand and the formamidinate ligand of another diruthenium unit (2.719 Å).

N–H···Cl interactions (2.513 Å) between two adjacent diruthenium units are found in the structure of **Ruamp**·Et_2O. These interactions are established through the axial chloride ligand of one unit and the equatorial amp ligand of a neighboring molecule. The same molecules are also connected through C–H···O interactions (2.535 Å) between a formamidinate of one molecule and the acetate of the second molecule. In addition, the diethyl ether solvent molecules interact with the diruthenium units through C–H···O interactions (2.602 Å) (Fig. 3b).

The diruthenium molecules found in the packing of the **Ru′hmp** structure are connected through two different C–H···O interactions. The first one is stablished between the O atom of a methoxy-group of one DAniF ligand and a H atom of the ring of the amp ligand of a neighboring unit (C···O distance of 2.377 Å), and the second one between the O atom of another formamidinate ligand and the acetate ligand of the adjacent molecule (C···O distance of 3.410 Å) (Fig. 3c).

In the structure of **Ru′amp**·0.5C_6H_{12}, the most relevant supramolecular interactions are N–H···Cl, which are established between the chloride axial ligand of molecule and the NH hydrogen from the amp ligand of the neighbor molecule (2.462 Å). These two molecules interact with other two diruthenium units through C–H···O interactions (C···O distance of 3.343 Å). In addition, C–H···O interactions are also observed between the methoxy-groups of the formamidinate ligands and the crystallization solvent molecules (2.661 Å) (Fig. 3d).

Variable temperature magnetization measurements (Fig. 4 and S11–S13†) were carried out on **Ruhmp**, **Ruamp**, **Ru′hmp**, and **Ru′amp**. The experimental $\chi_M T$ values at room temperature (Table 1) are similar or slightly larger than 1.87 cm^3 K mol^{-1}, the contribution expected for a $S = 3/2$ state ($g = 2$) that arises from a $\sigma^2\delta^2\pi^4(\delta^*\pi^*)^3$ electronic configuration. Cooling the sample results in a decrease of the $\chi_M T$ product, which is mainly ascribed to a strong zero-field splitting. Accordingly, the data were fitted considering a quadruplet

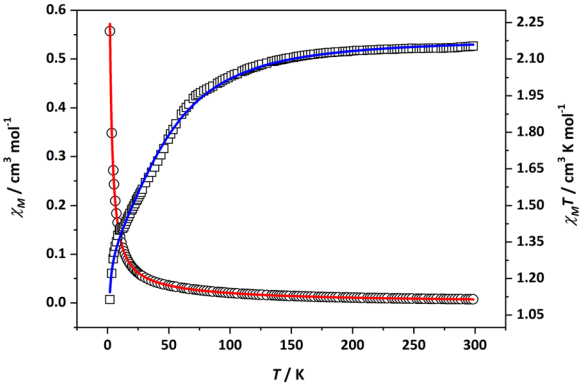

Fig. 4 Temperature dependence of the molar susceptibility χ_M (circles) and $\chi_M T$ (squares) for **Ru′hmp**. Solid lines are the best fit to the data as described in the text.

state undergoing an axial zero-field splitting (D) and an intermolecular magnetic exchange (zJ), which was included in the model as a perturbation on the molecular field (see Eqn. S1–S4†). Table 1 shows the parameters obtained from these fits. These parameters are similar to those obtained previously for related complexes.[21]

In order to design a suitable chiral platform for applications in solution, these complexes must show configurational stability. In this regard, the presence of only $[M–Cl]^+$ fragments in the ESI† data shows that the paddlewheel structure of these complexes is fairly stable. A potential racemization pathway of a single enantiomer would require, at least, a flip of the non-symmetric ligand or the exchange of two of its equatorial ligands. Previous studies showed that carboxylate ligands of diruthenium complexes can be released and replaced by other bridging ligands under acidic conditions, but higher donor character ligands such as formamidinates, hydroxypyridinates and aminopyridinates are certainly much less labile.[39–41] Nevertheless, the presence of other exchangeable-labile ligands is necessary to permit the formation of a substrate-catalyst complex for applications in catalysis. Indeed, diruthenium paddlewheel catalysts tested to date behave as Lewis acids, activated after removing their anionic halide ligand at the axial position.[26–28,42–44] Then, the coordination of new incoming ligands at any of the two axial positions in this type of complexes could be possible. However, this is probably not the case in this system because one of their axial positions is blocked by the methyl groups of hmp or amp ligands and, therefore, the configuration of the chiral center would be maintained after ligand exchange, which would allow a better control of the reaction stereochemistry. Moreover, it should be noted that this coordination of the incoming ligand would occur directly on a metal that is part of a stereogenic axis.

The UV-vis spectra of **Ruhmp**, **Ruamp**, **Ru′hmp**, and **Ru′amp** in dichloromethane solutions (Fig. 5a) show remarkable differences depending on the pyridinate ligand. The spectrum of complex **Ruhmp** shows a shoulder at 360 nm and two maxima at 505 and 627 nm, which are ascribed to

Table 1 Parameters obtained from the magnetic data of **Ruhmp**, **Ruamp**, **Ru′hmp**, and **Ru′amp**

Compound	**Ruhmp**	**Ruamp**	**Ru′hmp**	**Ru′amp**
$\chi_M T$ at 300 K (cm^3 K mol^{-1})	1.97	2.14	2.16	1.77
g	2.073(1)	2.121(2)	2.159(1)	1.959(1)
D (cm^{-1})	51.1(1)	34(1)	56.6(6)	59.2(6)
zJ (cm^{-1})	−0.04(1)	−0.38(3)	−0.149(8)	−0.057(7)
σ^2([a])	3.62×10^{-4}	1.27×10^{-3}	1.85×10^{-4}	1.31×10^{-4}

[a] $\sigma^2 = \Sigma(\chi_M T_{calc} - \chi_M T_{exp})^2/\Sigma(\chi_M T_{exp})^2$.

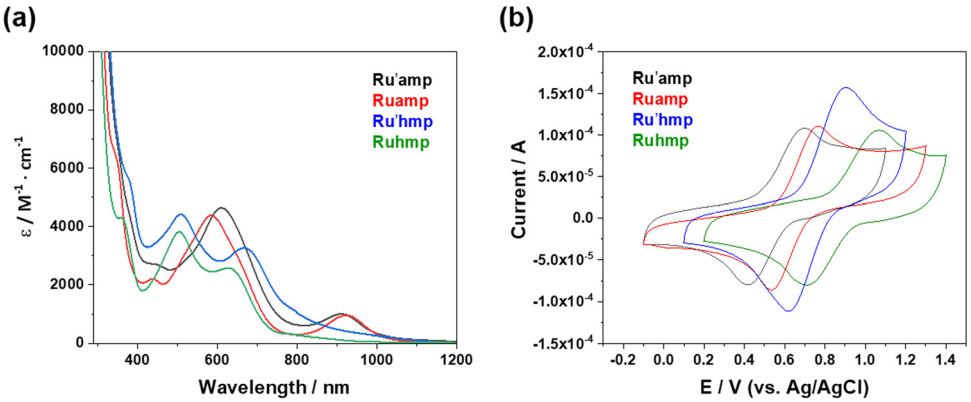

Fig. 5 (a) UV-vis spectra and (b) CV data of **Ruhmp** (green), **Ruamp** (red), **Ru′hmp** (blue) and **Ru′amp** (black) in dichloromethane solutions.

π(aryl) → π*(Ru_2), π*(Ru_2) → σ*(Ru_2/axial) and π(Ru–N/O,Ru_2) → δ*(Ru_2) transitions, respectively. In the spectrum of **Ruamp** more absorptions can be distinguished at 347 nm (sh), 437, 527 (sh), 585, 663 (sh) and 924 nm. They are assigned to π(aryl) → π*(Ru_2), π(N/O/aryl) → σ*(Ru_2/axial), π*(Ru_2) → σ*(Ru_2/axial), σ(Ru_2/axial) → π*(Ru_2), π(Ru–N/O,Ru_2) → δ*(Ru_2) and δ(Ru_2) → π*(Ru_2), respectively.[45] A slight general redshift in the absorptions for the complexes containing DAniF as formamidinate ligand compared with the DPhF counterparts is observed: 379 (sh), 509 and 668 nm for **Ru′hmp**, and 377 (sh), 448, 538 (sh), 610, 675 (sh) and 912 nm for **Ru′amp**.

Cyclic voltammetry data obtained using degassed tetrabutylammonium perchlorate 0.05 M dichloromethane solutions of the complexes (Fig. 5b) show a unique one-electron redox process within the cathodic and anodic limits of dichloromethane, which is assigned to the $Ru_2^{5+/6+}$ redox couple. This redox process is also observed in similar metal–metal bonded diruthenium complexes previously reported.[22] Table 2 shows the $E_{1/2}$ and ΔE values found for each complex. **Ru′amp** presents the lowest $E_{1/2}$ value, followed by **Ruamp**, **Ru′hmp** and **Ruhmp**. This tendency is given by the presence of different equatorial ligands. The presence of three *N*,*N*′-donor ligands (**Ruamp**, **Ru′amp**) leads to lower redox potential values for the oxidation process. Besides, complexes containing DAniF ligands (**Ru′amp**, **Ru′hmp**) exhibit lower values of $E_{1/2}$ when comparing with the DPhF analogues (**Ruamp**, **Ruhmp**). Thus, the higher the electron-richness of the diruthenium core, the lower is the $E_{1/2}$ value.

Table 2 Electrochemical data (V, *vs.* Ag/AgCl) from CV of **Ruhmp**, **Ru′hmp**, **Ruamp**, and **Ru′amp**

Compound	**Ruhmp**	**Ru′hmp**	**Ruamp**	**Ru′amp**
$E_{1/2}$	0.89	0.76	0.65	0.56
ΔE	0.36	0.28	0.23	0.28

Conclusions

Working with chiral complexes containing only achiral ligands permits easy access to a wide range of structural and electronic properties by using different functional groups around the metal centers, not limited by the available reagents from the chiral pool. The electronic spectroscopy and cyclic voltammetry data of the complexes herein presented show that a change of hmp by amp significantly affects both their electronic spectra and redox potentials. On the other hand, the change of formamidinate ligands permits a subtler modulation. Including other different substituents, even in remote positions of the ligands would permit the modulation of the electronic properties of this chiral scaffold and, therefore, the Lewis acidity of potential cationic complexes obtained after removal of their axial chloride.[46,47] We are currently starting to explore the chiral resolution of these configurationally stable compounds by chiral chromatography, and derivatization strategies to form a separable diastereomeric mixtures. This would open novel perspectives not only in the field of asymmetric synthesis,

but also in the study of other properties such as non-linear optics or magnetochiral effects.

Data availability

The data supporting this article have been included as part of the ESI.† CCDC 2384530–2384533 contains the crystallographic data for this paper.

Author contributions

Isabel Coloma: investigation, data curation, formal analysis, writing-review and editing. Santiago Herrero: formal analysis, writing-review and editing. Miguel Cortijo: conceptualization, formal analysis, supervision, writing-original draft, writing-review and editing.

Conflicts of interest

There are no conflicts to declare.

Acknowledgements

This research was funded by the Universidad Complutense de Madrid (GRFN32/23, GRFN24/24 and PR3/23-30828). I. Coloma acknowledges predoctoral grant from the Complutense University of Madrid and Banco Santander (CT82/20-CT83/20). We also thank Elena García-Chamocho for her help with cyclic voltammetry measurements.

References

1 E. B. Bauer, *Chem. Soc. Rev.*, 2012, **41**, 3153–3167.
2 M. Diéguez, *Chiral Ligands: Evolution of Ligand Libraries for Asymmetric Catalysis*, CRC Press, Boca Raton, 1st edn, 2021.
3 Z.-Y. Cao, W. D. G. Brittain, J. S. Fossey and F. Zhou, *Catal. Sci. Technol.*, 2015, **5**, 3441–3451.
4 J. Ma, X. Zhang, X. Huang, S. Luo and E. Meggers, *Nat. Protoc.*, 2018, **13**, 605–632.
5 Z. Zhou, S. Chen, Y. Hong, E. Winterling, Y. Tan, M. Hemming, K. Harms, K. N. Houk and E. Meggers, *J. Am. Chem. Soc.*, 2019, **141**, 19048–19057.
6 P. Dey, P. Rai and B. Maji, *ACS Org. Inorg. Au*, 2022, **2**, 99–125.
7 P. S. Steinlandt, L. Zhang and E. Meggers, *Chem. Rev.*, 2023, **123**, 4764–4794.
8 C.-X. Ye and E. Meggers, *Acc. Chem. Res.*, 2023, **56**, 1128–1141.
9 C. Bartual-Murgui, L. Piñeiro-López, F. J. Valverde-Muñoz, M. C. Muñoz, M. Seredyuk and J. A. Real, *Inorg. Chem.*, 2017, **56**, 13535–13546.
10 A. Verma, K. Tomar and P. K. Bharadwaj, *Inorg. Chem.*, 2017, **56**, 13629–13633.
11 M. Cortijo, C. Viala, T. Reynaldo, L. Favereau, I. Fabing, M. Srebro-Hooper, J. Autschbach, N. Ratel-Ramond, J. Crassous and J. Bonvoisin, *Inorg. Chem.*, 2017, **56**, 4555–4567.
12 Á. Valentín-Pérez, A. Naim, E. Hillard, P. Rosa and M. Cortijo, *Polymer*, 2018, **10**, 311.
13 A. Srinivasan, M. Cortijo, V. Bulicanu, A. Naim, R. Clérac, P. Sainctavit, A. Rogalev, F. Wilhelm, P. Rosa and E. A. Hillard, *Chem. Sci.*, 2018, **9**, 1136–1143.
14 J.-H. Huang, X.-Y. Dong, Y.-J. Wang and S.-Q. Zang, *Coord. Chem. Rev.*, 2022, **470**, 214729.
15 J. Amin and C. J. Richards, *Chem. Commun.*, 2012, **48**, 10192.
16 R. Jouhannet, S. Dagorne, A. Blanc and P. De Frémont, *Chem. – Eur. J.*, 2021, **27**, 9218–9240.
17 N. Lefringhausen, V. Seiffert, C. Erbacher, U. Karst and J. Müller, *Chem. – Eur. J.*, 2023, **29**, e202202630.
18 S. Herrero and M. A. Usón, *J. Chem. Educ.*, 1995, **72**, 1065.
19 M. A. S. Aquino, *Coord. Chem. Rev.*, 1998, **170**, 141–202.
20 M. A. S. Aquino, *Coord. Chem. Rev.*, 2004, **248**, 1025–1045.
21 M. Cortijo, R. González-Prieto, S. Herrero, J. L. Priego and R. Jiménez-Aparicio, *Coord. Chem. Rev.*, 2019, **400**, 213040.
22 E. Van Caemelbecke, T. Phan, W. R. Osterloh and K. M. Kadish, *Coord. Chem. Rev.*, 2021, **434**, 213706.
23 S. Su, X. Zhu, Y. Wen, L. Zhang, Y. Yang, C. Lin, X. Wu and T. Sheng, *Angew. Chem., Int. Ed.*, 2019, **58**, 15344–15348.
24 G. M. Chiarella, F. A. Cotton, C. A. Murillo, K. Ventura, D. Villagrán and X. Wang, *J. Am. Chem. Soc.*, 2014, **136**, 9580–9589.
25 J. Zhang, W. Kosaka, Y. Kitagawa and H. Miyasaka, *Angew. Chem., Int. Ed.*, 2022, **61**, e202115976.
26 T. Miyazawa, T. Suzuki, Y. Kumagai, K. Takizawa, T. Kikuchi, S. Kato, A. Onoda, T. Hayashi, Y. Kamei, F. Kamiyama, M. Anada, M. Kojima, T. Yoshino and S. Matsunaga, *Nat. Catal.*, 2020, **3**, 851–858.
27 K. Makino, Y. Kumagai, T. Yoshino, M. Kojima and S. Matsunaga, *Org. Lett.*, 2023, **25**, 3234–3238.
28 J. K. Sailer, J. C. Sharland, J. Bacsa, C. F. Harris, J. F. Berry, D. G. Musaev and H. M. L. Davies, *Organometallics*, 2023, **42**, 2122–2133.
29 A. Inchausti, A. Terán, A. Manchado-Parra, A. De Marcos-Galán, J. Perles, M. Cortijo, R. González-Prieto, S. Herrero and R. Jiménez-Aparicio, *Dalton Trans.*, 2022, **51**, 9708–9719.
30 P. A. Angaridis, F. A. Cotton, C. A. Murillo, A. S. Filato and M. A. Petrukhina, in *Inorganic Syntheses*, ed. G. S. Girolami and A. P. Sattelberger, Wiley, 1st edn, 2014, pp. 114–121.
31 W.-Z. Chen and T. Ren, *Inorg. Chem.*, 2006, **45**, 8156–8164.
32 K. B. Gan, R.-L. Zhong, Z.-W. Zhang and F. Y. Kwong, *J. Am. Chem. Soc.*, 2022, **144**, 14864–14873.
33 Y. Chen, L. Liu, C. Chen, Y. Liu, B. Zhou, X. Lu, Z. Xu and L. Ye, *Angew. Chem., Int. Ed.*, 2023, **62**, e202303670.
34 A. C. Gehrold, T. Bruhn and G. Bringmann, *J. Org. Chem.*, 2016, **81**, 1075–1088.
35 O. V. Dolomanov, L. J. Bourhis, R. J. Gildea, J. A. K. Howard and H. Puschmann, *J. Appl. Crystallogr.*, 2009, **42**, 339–341.
36 G. M. Sheldrick, *Acta Crystallogr., Sect. A: Found. Adv.*, 2015, **71**, 3–8.
37 G. M. Sheldrick, *Acta Crystallogr., Sect. C: Struct. Chem.*, 2015, **71**, 3–8.
38 E. Pretsch, P. Bühlmann and M. Badertscher, *Structure determination of organic compounds: tables of spectral data*, Springer, Berlin, 4th edn, 2009.

39 I. Coloma, M. Cortijo, I. Fernández-Sánchez, J. Perles, J. L. Priego, C. Gutiérrez, R. Jiménez-Aparicio, B. Desvoyes and S. Herrero, *Inorg. Chem.*, 2020, **59**, 7779–7788.
40 I. Coloma, M. Cortijo, M. J. Mancheño, M. E. León-González, C. Gutierrez, B. Desvoyes and S. Herrero, *Inorg. Chem. Front.*, 2023, **10**, 4402–4413.
41 I. Coloma, J. Parrón-Ballesteros, M. Cortijo, C. Cuerva, J. Turnay and S. Herrero, *Inorg. Chem.*, 2024, **63**, 12870–12879.
42 J. E. Barker and T. Ren, *Inorg. Chem.*, 2008, **47**, 2264–2266.
43 H. B. Lee and T. Ren, *Inorg. Chim. Acta*, 2009, **362**, 1467–1470.
44 N. Komiya, T. Nakae, H. Sato and T. Naota, *Chem. Commun.*, 2006, 4829.
45 A. Inchausti, R. Mollfulleda, M. Swart, J. Perles, S. Herrero, V. G. Baonza, M. Taravillo and Á. Lobato, *Adv. Sci.*, 2024, **11**, 2401293.
46 C. Lin, T. Ren, E. J. Valente, J. D. Zubkowski and E. T. Smith, *Chem. Lett.*, 1997, **26**, 753–754.
47 T. Ren, *Coord. Chem. Rev.*, 1998, **175**, 43–58.